The effect of internal impurities on the mechanical and conductance properties of gold nanowires during elongation

2013 Modelling Simul. Mater. Sci. Eng. 21 025004

(http://iopscience.iop.org/0965-0393/21/2/025004)

Modelling Simul. Mater. Sci. Eng. **21** (2013) 025004 (8pp) doi:10.1088/0965-0393/21/2/025004

The effect of internal impurities on the mechanical and conductance properties of gold nanowires during elongation

S Barzilai[1], **F Tavazza and L E Levine**

Material Measurement Laboratory, National Institute of Standards and Technology, 100 Bureau Drive, Stop 8553, Gaithersburg, MD 20899, USA

Received 27 September 2012, in final form 28 November 2012
Published 24 January 2013
Online at stacks.iop.org/MSMSE/21/025004

Abstract

The conductance and mechanical properties of contaminated gold nanowires (NWs) were studied using first principle calculations. Nanowires containing internal impurities of H_2O or O_2 were elongated along two different directions. It was found that both impurities interact with the gold atoms and affect the properties of the NWs. From a mechanical viewpoint, the impurities increase the bond strength in their vicinity and, throughout the entire elongation, remain surrounded by gold atoms. The impurities do not migrate to the surface and never end up in the single atom chain. The NW fracture always occurs at an Au–Au bond, far from the impurity. Therefore, the impurities do not affect the fracture strength but do decrease the strain at fracture. A variety of conductance effects were observed depending on the type and location of the impurity, and the O_2 has the most significant impact. The O_2 reduces the conductance when it is close to the gold atoms in the main pathway. However, at the late stages of the elongation, both impurities are located far from the main pathway and have little influence on the conductance.

(Some figures may appear in colour only in the online journal)

1. Introduction

Gold nanowires (NWs) are extremely ductile and can be thinned down to single atom chains (SACs) during tensile deformation. This unusual ability makes them good candidates for applied fields such as nanoelectronics and also attractive from a basic science viewpoint. Many experimental studies [1–16] have been carried out to characterize the conductance of gold nanowires during elongation. In our experimental system [13, 14, 16], the sample is created in a high vacuum chamber, at ≈4 K, by 'crashing' the tip of a gold wire onto a flat gold plate to form a metallic contact junction. A nanowire is then formed by drawing the wire

[1] On sabbatical leave from the Nuclear Research Center Negev.

away from the plate. Conductance is measured continuously during wire thinning. When the conductance decreases to 1 G_0 (where $G_0 = 2e^2/h$, with e the electron charge and h Planck's constant) the general conclusion is that part of the NW has thinned to a SAC.

To verify this interpretation, many theoretical studies have been published to explain the structural changes that occur during gold NW elongation and determine the effect of these configurations on the conductance [17–34]. Indeed, it was found that during the elongation, the arrangement of the gold atoms changes from three-dimensional (3D) phases to a variety of two-dimensional (2D) phases and finally to SACs, which elongate gradually from one up to about nine atoms in the chain. When part of the NW becomes a SAC, the conductance goes to $\approx 1\ G_0$. However, in our experimental system and in other common apparatuses that measure the conductance (mechanically controlled break junctions and scanning probe microscopes), contamination on the Au tip and plate can be trapped in the contact junction to form an internal contaminant, or contaminants can migrate along the nanowire surface during the elongation. Both types of impurities can influence the conductance measurement, and cast doubt upon the straightforward link between 1 G_0 conductance and SAC formation.

Despite the importance of this issue, almost no studies have been published on the role of internal and external impurity migration on the conductance of 3D NWs during elongation. The only exception we found is the work of Jelinek *et al* [35] that assumes hydrogen and oxygen dissociation, and computes the conductance of a gold NW in the presence of these atomic species on the NW surface. The rest of the theoretical studies that investigate the effect of impurities consider only the structural effect on a 3D gold NW elongation [36, 37], or calculate the effect of pre-placed impurities on a SAC [38–50], neglecting the original position of the impurities prior to the elongation and without considering how the contamination can reach the SAC zone.

To study the effect of internal contaminants on the structure and conductance of gold NWs during elongation, we selected H_2O and O_2 as common contaminants that may exist in the experimental apparatus, and simulated the deformation of several gold NWs containing these internal impurities. Understanding the mechanisms that control the conductance in atomic-scale wires and the effect of the impurities is important both from a basic science standpoint and for applications in nanoelectronics and nano-devices.

2. Methodology

The calculations performed to elongate the nanowires were carried out in the framework of density functional theory (DFT) using the DMol^{3}code[2] [51, 52]. This code employs localized basis sets, which make them fast and particularly well suited for cluster calculations. We used a real-space cutoff of 4 Å and a double-zeta, atom-centered basis set (dnd). The exchange-correlation potential was treated within the Perdew–Burke–Ernzerhof (PBE) generalized gradient approximation (GGA) approach [53]. The ion core electrons of the Au were described by a hardness conserving semilocal pseudopotential (dspp) [54]; only the outer electrons ($5s^2 5p^6 5d^{10} 6s^1$) were treated as valence electrons. To ensure that the results of the calculations are directly comparable, identical conditions were employed for all systems. The geometry optimization was performed using a conjugate gradient approach based on a delocalized internal coordinate scheme [55, 56]. The system was considered converged when the change in total energy dropped below 10^{-3} eV (5×10^{-5} Ha) and the maximum displacement dropped below 10^{-4} Å.

[2] Commercial software is identified to specify procedures. Such identification does not imply recommendation by the National Institute of Standards and Technology.

The conductance calculations were performed at zero bias using a non-equilibrium Green's function technique based on the Landauer formalism [57], as implemented in the ATK package [23, 58, 59]. The system was divided into three regions: the left and right Au electrodes and the central scattering region. For the latter, we used the atomic configurations obtained by the DFT elongation. The attachment of the electrodes to the scattering zone was completely seamless since the grip atoms in the deformation simulations had been kept fixed in ideal face-centered cubic positions. Huckel tight binding [60] was utilized for all of the cluster-based configurations (retrieved from the DFT simulations) using the Cerda [61] and Hoffmann [62] parametrization for the Au and for the O and H atoms, respectively.

Pure Au NWs containing 115 atoms oriented with (1 1 0) planes perpendicular to the Z (wire) axis, and contaminated gold NWs having the same orientation, were elongated along two directions: 6° off the Z-axis, to arbitrarily represent a small misalignment as in most of the tensile experiments, and 48° off the Z-axis, to represent an arbitrary, much larger misalignment. At each tensile step, the grip atoms (two layers at each end of the wire) were translated by a fixed amount and then kept fixed, while all the other atoms were allowed to relax into a new configuration. For more detailed information, see [17].

3. Results

To simulate internal contamination in the contact junction, one of the internal Au atoms was replaced by an O_2 or H_2O impurity. In this study, we considered two different sites: in the center of the NW and in the shoulder adjacent to the rigid grip layers. Prior to the elongation, for each site and each impurity, three initial impurity orientations were selected for relaxation. After the relaxations, all of the initial orientations were changed and converged to a single orientation which was identical for both the central and the shoulder sites. The O_2 was relaxed to the middle of its site and become oriented ≈45° to the Z-axis, while the H_2O moved from the center and attached to one of the Au atoms above it. These relaxed structures were used as initial configurations for the NW elongation.

Figure 1 shows the computed conductance as a function of elongation for two representative simulations where the contaminant (O_2 in figure 1(*a*) and H_2O in figure 1(*b*)) is located initially in the wire center. For comparison, the dashed curves show the conductance of the corresponding pure Au nanowires. The angle of the strain axis with respect to the Z-axis was 6° in figure 1(*a*) and 48° in figure 1(*b*). Snapshots of the contaminated nanowires are present at the bottom of the figure. The simulation results demonstrate that impurities can affect both the structural evolution and the conductance, depending on the type and location of the impurity. To separate these effects, the conductance of each elongated NW was calculated at every elongation step both *with* the impurity (solid symbols) and with the impurity removed (hollow symbols). When the impurity is removed, no structural relaxations are carried out, allowing the 'chemical' contribution of the impurity to be evaluated. The rest of the simulations, where the impurities are located in the shoulder or have different elongation directions, exhibit similar impurity effects and are summarized in table 1.

Both impurities had similar effects on the structural evolution, but different effects on the conductance properties. During the entire elongation, the impurity strengthens the local atomic bonding and the impurity remains completely surrounded by gold atoms. Thus, the phase transformations from 3D to 2D, and afterward to the SAC, occur far from the impurity site. This strengthening effect decreases the 3D to 2D transformation strain by ≈50%, and thus, also decreases the fracture strain. Since the impurities are far from the fracture sight, they do not affect the fracture strength. The fracture strength and its standard deviation for contaminated Au NWs is (1.55 ± 0.09) nN; this is unchanged (within the uncertainties) from

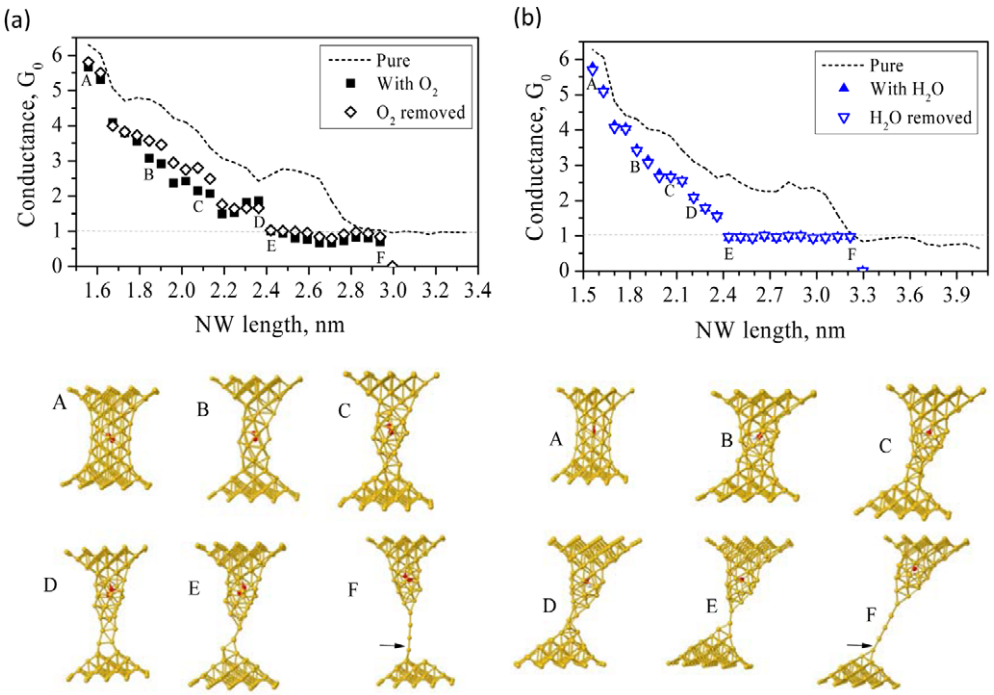

Figure 1. The computed conductance of the gold NWs during elongation. The short dashed curves represent the conductance of the pure NWs. The solid symbols represent the presence of an O_2 (*a*) and H_2O (*b*) impurity in the center of the NW. The hollow symbols refer to the same atomic configuration of the gold atoms, but without the impurities. The arrows indicate the fracture location.

the previously computed result [17] of (1.54 ± 0.06) nN for pure Au nanowires and from the experimental value of (1.5 ± 0.3) nN observed previously [63].

The initial position of the impurity plays a crucial role in the conductance evolution. Impurities that are initially located in the shoulder of the NW simply strengthen that side of the wire; the conductance is governed by the structural changes that occur during thinning of the rest of the wire. As can be seen in table 1, when the impurities were initially located in the shoulder, the minimal conductance calculated at each structural configuration was similar to that found for the pure NWs. Moreover, when the impurity is removed (with no relaxation), the change in conductance is negligible. This behavior does not imply that the impurities have no effect on the local conductance or electronic structure, merely that there are so many conductance channels available in this thick part of the wire that the conductance bottleneck exists elsewhere.

In contrast, the centrally located impurities reside in a thinner part of the wire, allowing the differences in chemical reactivity of the species to be readily apparent (see figure 1). Removing the H_2O molecule, while keeping the Au atoms in fixed positions, has no effect on the conductance. In contrast, removing the O_2 molecule substantially increases the conductance for NW length between 1.8 and2.1 nm. Here, the O_2 affects the main conductance channels. At larger strains, the wire away from the contaminant transforms to 2D and to SAC phases, and the total conductance is governed by this new bottleneck, similar to what was observed in the shoulder case.

Table 1. Mechanical characterization and conductance properties of pure and impure gold NWs.

Impurity (tensile direction—deviation from the Z-axis)	Fracture strength[a] (nN)	Transformation strain[b] [%] (NW Length (nm))			The minimal conductance[c] [G_0]			The maximal chemical effect[d] [G_0]		
		2D	SAC	Fracture	3D	2D	SAC	3D	2D	SAC
Pure(6°)	1.54 ± 0.06	80(2.7)	84(2.8)	123(3.3)	2.4	1.8	0.91	—	—	—
Pure(48°)		109(3.1)	114(3.2)	175(4.0)	2.2	1.6	0.65	—	—	—
O_2-Center(6°)	1.46	46(2.2)	61(2.4)	100(2.9)	2.1	1.5	0.67	−0.65	−0.25	−0.16
O_2-Center(48°)	1.46	52(2.3)	72(2.6)	124(3.3)	2.3	1.3	0.89	−0.44	−0.08	−0.03
O_2-Shoulder(6°)	1.55	42(2.1)	57(2.4)	77(2.7)	2.6	1.4	0.94	−0.29	0.05	0.03
O_2-Shoulder(48°)	1.73	62(2.4)	83(2.7)	141(3.6)	2.2	1.4	0.63	−0.30	0.04	0.04
H_2O-Center(6°)	1.63	50(2.2)	54(2.3)	107(3.1)	2.1	1.7	0.95	0.15	0.00	0.05
H_2O-Center(48°)	1.49	47(2.2)	62(2.4)	120(3.3)	2.5	1.6	0.92	0.09	0.00	−0.04
H_2O-Shoulder(6°)	1.58	34(2.0)	42(2.1)	73(2.6)	2.2	1.5	0.92	0.21	0.10	−0.06
H_2O-Shoulder(48°)	1.46	47(2.2)	57(2.4)	104(3.0)	2.2	1.7	0.83	0.13	0.02	0.02

[a] The fracture strength was computed by dividing the difference between the total energy of the NW at the iteration of the breakage and the previous one, by the change in the NW length caused by this step.
[b] The engineering strain at which the NW transforms to 2D, to SAC and when it breaks. The strain was computed by dividing the change in the NW length by the initial length.
[c] The minimum conductance that was calculated for the NW when the atomic arrangement of the Au atoms was in 3D, 2D and SAC phases.
[d] The maximal chemical effect is given by the maximal conductance difference between the NW that includes the impurity inside and the identical NW structure with the impurity removed.

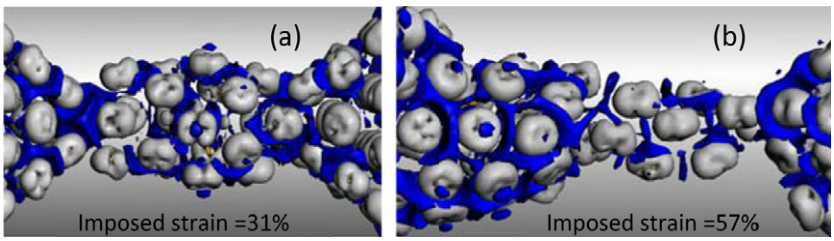

Figure 2. The iso-surface of the differential electron density of a gold NW containing an O_2 impurity in the center (*a*) and in the shoulder (*b*) of the NW. The dark (blue) and the light (gray) shades represent an increase and a decrease in the differential electron density by 10^{-2} e Å^{-3}, respectively.

The effect of O_2 and H_2O impurities on the conductance is summarized as the maximal chemical effect shown in table 1. To better understand this influence on the conductance, the differential electron densities (an electron density corresponds to the increase and decrease in the electron density relative to the individual atoms) and the transmission pathways were computed for a variety of cases of pure and contaminated gold NWs. Representative results of these properties are shown in figures 2 and 3 for gold NWs with the O_2 impurity in the center and in the shoulder.

Figure 2 shows the differential electron density for gold NWs containing an O_2 impurity in the center and in the shoulder. The observed differential density is distributed between the gold atoms in a non-uniform manner and may reflect the electron availability for conduction. For the NW with the central impurity (figure 2(*a*)), the differential electron density is highest between the atoms that are far from the impurity, and lowest between the atoms near the impurity. A different tendency was found for the NW that contains O_2 in the shoulder. In these

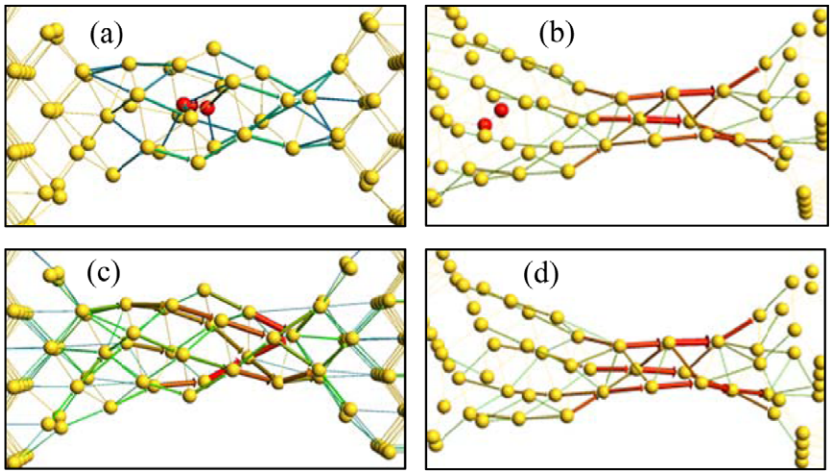

Figure 3. Transmission pathways at zero bias at the Fermi level for gold NWs elongated in the following states: (*a*) elongated to 20% with O_2 in the center, (*b*) elongated to 57% with O_2 in the shoulder, (*c*) and (*d*) correspond to the configurations computed in (*a*) and (*b*), respectively, but without the O_2. The thickness and the colors of the arrows are related to the level of the local current between each pair of atoms and are normalized to the maximal value in each figure.

simulations, the highest differential electron density was found between the gold atoms near the impurity, and the lowest between the atoms far from the impurity, in the thinning region of the NW (figure 2(*b*)). Further calculations of gold NWs with the same atomic configurations but without the O_2 indicate that in the vicinity of the O_2, the impurity causes small electron density depletion from the region between the gold atoms. This small depletion may be critical for the NW conductance if the impurity is located in a conduction bottleneck.

Representative transmission pathways for the NWs shown in figure 2 are presented in figure 3, along with the pathways from the NWs with the impurities removed. Small levels of conductance current were computed for the channels around the O_2 located in the center (figure 3(*a*)) and in the shoulder (figure 3(*b*)) of the NW. This small level of conductance can be related to the configuration of the gold atoms or to the interaction with the impurity. When the O_2 was artificially removed from the NWs, the capacity of the conductance channels was increased for the NW that had O_2 in the center (figure 3(*c*)), but almost no changes were obtained for the NW that had it in the shoulder (figure 3(*d*)).

The electron density and conductance transmission pathway results elucidate the chemical effect of the impurities. The H_2O has a negligible effect on the conductance and the O_2 has a much higher impact. When the O_2 is located in a region that limits the conductance due to the configuration of the metallic atoms, it further decreases the conductance. However, when it is far from such bottleneck configuration, it has only a small chemical effect on the conductance. In general, negligible changes in the conductance current around the impurities were observed for all of the simulations with an H_2O impurity and for the simulations that contained O_2 in the NW shoulder.

4. Summary and conclusions

The effect of internal H_2O and O_2 contaminants on the conductance of gold NWs was studied. All of the simulations show that, during the elongation, the impurities interact with the gold,

strengthen the atomic bonds in their vicinity and remain surrounded by gold atoms throughout the entire thinning process. These impurities stay inside the gold NW and never end up on the surface of the wire or in the actively thinning region. The location of the fracture occurs far from the impurities where the NW transforms first to 2D configurations and then to a SAC structure. Thus, the presence of these impurities does not affect the fracture strength of the NWs, but does reduce the fracture strain.

Removing the impurity without changing the atomic structure allowed us to evaluate the chemical effect of the impurity. In all cases examined, removing the H_2O impurity had no significant effect on the conductance. This was true even when the H_2O was located near the main transmission pathway. In contrast, an O_2 impurity has a substantial effect on the local transmission channels which can affect the total conductance of the NW. For the O_2 located in the shoulder, there is almost no effect on the conductance since the bottleneck is the thinning part of the wire which is well away from the impurity. For the centrally located O_2, during the early stages of plastic deformation, electron depletion partially closes the main transmission pathway, decreasing the conductance by around $0.44\,G_0$ to $0.65\,G_0$. As the NW changes its atomic configuration and transforms to a 2D phase and then a SAC, the bottleneck shifts to this part of the wire and the effect of the impurity on the conductance disappears.

The local strengthening of the atomic bonds near the impurity is the primary factor that prevents the impurity from being incorporated into the thinnest part of the deforming wire, thus limiting the impurity's effect on the conductance. This behavior may be different for an impurity located on the NW surface since its geometric configuration on the surface would allow the metallic Au–Au bonding to be broken with little effect on the Au–impurity bonding. Under those circumstances, the local strengthening would be greatly diminished, therefore allowing thinning of the wire in the vicinity of the impurity. However, to get a more complete understanding, this topic should be further investigated.

References

[1] Yanson I K, Shklyarevskii O I, Csonka Sz, van Kempen H, Speller S, Yanson A I and van Ruitenbeek J M 2005 *Phys. Rev. Lett.* **95** 256806
[2] Kiguchi M, Konishi T and Murakoshi K 2006 *Phys. Rev.* B **73** 125406
[3] Kiguchi M, Konishi T, Tasegawa K, Shidara S and Murakoshi K 2008 *Phys. Rev.* B **77** 245421
[4] Kiguchi M, Djukic D and van Ruitenbeek J M 2007 *Nanotechnology* **18** 035205
[5] Suzuki R, Tsutsui M, Miura D, Kurokawa S and Sakai A 2007 *Japan. J. Appl. Phys.* **46** 3694
[6] Kizuka T 2008 *Phys. Rev.* B **77** 155401
[7] Oshima Y, Kurui Y and Takayanagi K 2010 *J. Phys. Soc. Japan.* **79** 054702
[8] Scheer E *et al* 1998 *Nature* **394** 154
[9] Kurui Y, Oshima Y, Okamoto M and Takayanagi K 2009 *Phys. Rev.* B **79** 165414
[10] Smit R H M, Untiedt C, Rubio-Bollinger G, Segers R C and van Ruitenbeek J M 2003 *Phys. Rev. Lett.* **91** 076805
[11] Dreher M, Pauly F, Heurich J, Cuevas J C, Scheer E and Nielaba P 2005 *Phys. Rev.* B **72** 75435
[12] Ohnishi H, Kondo Y and Takayanagi K 1998 *Nature* **395** 780
[13] Smith D T, Pratt J R, Tavazza F, Levine L E and Chaka A M 2010 *J. Appl. Phys.* **107** 084307
[14] Thijssen W H A, Marjenburgh D, Bremmer R H and van Ruitenbeek J M 2006 *Phys. Rev. Lett.* **96** 26806
[15] Tavazza F, Smith D T, Levine L E, Pratt J R and Chaka A M 2011 *Phys Rev. Lett.* **107** 126802
[16] Smith D T, Pratt J R and Howard L P 2009 *Rev. Sci. Instrum.* **80** 035105
[17] Tavazza F, Levine L E and Chaka A M 2009 *J. Appl. Phys.* **106** 43522
[18] Agraıt N, Yeyati A L and van Ruitenbeek J M 2003 *Phys. Rep.* **377** 81
[19] Agraıt N, Rubio G and Vieira S 1995 *Phys. Rev. Lett.* **74** 3995
[20] Rubio-Bollinger G, Joyez P and Agraıt N 2004 *Phys. Rev. Lett.* **93** 11680
[21] Nitzan A and Ratner M A 2003 *Science* **300** 1384
[22] Qian Z, Li R, Hou S, Xue Z and Sanvito S 2007 *J. Chem. Phys.* **127** 194710
[23] Brandbyge M, Mozoz J L, Ordejon P, Taylor J and Stokbro K 2002 *Phys. Rev.* B **65** 165401
[24] Fujimoto Y and Hirose K 2003 *Phys. Rev.* B **67** 195315

[25] Lee Y J *et al* 2004 *Phys. Rev.* B **69** 125409
[26] Zhuang M and Ernzerhof M 2004 *J. Chem. Phys.* **120** 4921
[27] Grigoriev A *et al* 2006 *Phys. Rev. Lett.* **97** 236807
[28] Tavazza F, Levine L E and Chaka A M 2010 *Phys. Rev.* B **81** 235424
[29] Ke L *et al* 2007 *Nanotechnology* **18** 095709
[30] Grigoriev A, Skorodumova N V, Simak S I, Wendin G, Johansson B and Ahuja R 2010 *Phys. Rev. Lett.* **97** 236807
[31] Szczesniak D and Khater A 2012 *Eur. Phys. J.* **85** 174
[32] Kwapinski T 2010 *J. Phys.: Condens. Matter* **22** 295303
[33] Shiota T, Mares A I, Valkering A M C, Oosterkamp T H and van Ruitenbeek J M 2008 *Phys. Rev.* B **77** 125411
[34] Robio-Bollinger G, de las Heras C, Bascones E, Agrait N, Guinea F and Vieira S 2003 *Phys. Rev.* B **67** 12140
[35] Jelínek P, Prez R, Ortega J and Flores F 2008 *Phys. Rev.* B **77** 115447
[36] Anglada E, Torres J A, Yndurain F and Soler J M 2007 *Phys. Rev. Lett.* **98** 096102
[37] Tavazza F, Levine L E and Chaka A M 2012 *Comput. Theor. Chem.* **987** 84
[38] Novaes F D, da Silva A J R, da Silva E Z and Fazzio A 2006 *Phys. Rev. Lett.* **96** 016104
[39] da Silva E Z, Novaes F D, da Silva A J R and Fazzio A 2006 *Nanoscale Res. Lett.* **1** 91
[40] Ishida H 2007 *Phys. Rev.* B **75** 205419
[41] Ishida H 2008 *Phys. Rev.* B **77** 155415
[42] Skorodumova N V and Simak S I 2003 *Phys. Rev.* B **67** 121404 (R)
[43] Skorodumova N V, Simak S I, Kochetov A E and Johansson B 2007 *Phys. Rev.* B **75** 235440
[44] Legoas S B, Rodrigues V, Ugarte D and Galvao D S 2004 *Phys. Rev. Lett.* **93** 216103
[45] Velez P, Dassie S A and Leiva E P M 2010 *Phys. Rev.* B **81** 125440
[46] Hobi E Jr, Fazzio A and da Silva A J R 2008 *Phys. Rev. Lett.* **100** 056104
[47] Kochetov A E and Mikhaylushkin A S 2008 *Eur. Phys. J.* **61** 441
[48] Zhang C, Barnett R N and Landman U 2008 *Phys. Rev. Lett.* **100** 046801
[49] Barnett R N, Hkkinen H, Scherbakov A G and Landman U 2004 *Nano Lett.* **4** 1845
[50] Bahn S R, Lopez N, Norskov J K and Jacobsen K W 2002 *Phys. Rev.* B **66** 081405
[51] Delley B 1990 *J. Chem. Phys.* **92** 508
[52] Delley B 2000 *J. Chem. Phys.* **113** 7756
[53] Perdew J P, Burke S and Ernzerhof M 1996 *Phys. Rev. Lett.* **77** 3865
[54] Delley B 2002 *Phys. Rev.* B **66** 155125
[55] Pulay P and Fogarasi G 1992 *J. Chem. Phys.* **96** 2856
[56] Baker J, Kessi A and Delley B 1996 *J. Chem. Phys.* **05** 192
[57] Nazarov Y V and Blanter Ya M 2009 *Quantum Transport: Introduction to Nanoscience* (Cambridge: Cambridge University Press)
[58] Atomistix ToolKit version 10.02, QuantumWise A/S
[59] Taylor J, Guo H and Wang J 2001 *Phys. Rev.* B **63** 245407
[60] Stokbro K *et al* 2010 *Phys. Rev.* B **82** 75420
[61] Cerda J and Soria F 2000 *Phys. Rev.* B **61** 7965
[62] Ammeter J H, Burgi H B, Thibeault J C and Hoffmann R 1978 *J. Am. Chem. Soc.* **100** 3686
[63] Robio-Bollinger G, Bahn S R, Agrait N, Jacobsen K W and Vieria S 2001 *Phys. Rev. Lett.* **87** 26101